Atmos. Chem. Phys. Discuss., 6, 13001–13025, 2006
www.atmos-chem-phys-discuss.net/6/13001/2006/

Atmospheric Chemistry and Physics Discussions

A numerical study of tropical cross-tropopause transport by convective overshoots during the TROCCINOX golden day

J.-P. Chaboureau[1], J.-P. Cammas[1], J. Duron[1], P. J. Mascart[1], N. M. Sitnikov[2], and H.-J. Voessing[3]

[1]Laboratoire d'Aérologie, Université Paul Sabatier and CNRS, Toulouse, France
[2]Central Aerological Observatory, Dolgoprudny, Russia
[3]Institute for Atmospheric Physics, University of Mainz, Germany

Received: 20 November 2006 – Accepted: 5 December 2006 – Published: 12 December 2006

Correspondence to: J.-P. Chaboureau (jean-pierre.chaboureau@aero.obs-mip.fr)

Abstract

Observations obtained during the Tropical Convection, Cirrus and Nitrogen Oxides (TROCCINOX) golden day have revealed the presence of ice particles up to 410 K (18.2 km) 2 km above the local tropopause. The case is investigated using a three-dimensional quadruply nested non-hydrostatic simulation and Meteosat Second Generation (MSG) observations. The simulation fairly well reproduces the measurements along the flight track. A reasonable agreement with MSG observations is also achieved: the 10.8-µm brightness temperature (BT) minimum of 187 K is reproduced (a value 6 K colder than the environmental cold-point temperature) as well as the positive BT difference between the 6.2- and 10.8-µm bands, an overshoot signature. The simulation produces several overshooting plumes up to 410 K yielding an upward transport of water vapour of a few tons per second across the tropical tropopause. The estimated mass flux agree with those derived from over tracer budgets indicating that convection transport mass across the tropopause.

1 Introduction

The water vapour transport across the Tropical Tropopause Layer (TTL) is a key process for interpreting the observed increase in stratospheric water vapour of about 1% per year (Oltmans et al., 2000; Rosenlof et al., 2001), influencing the ozone layer and climate change. Half of increase in stratospheric water vapour is attributed to changes in methane and its oxidation (Etheridge et al., 1998) while the other half is believed to be due to water vapour transport across the tropical tropopause. In the TTL, the water vapour transport is controlled by the cold point, the coldest temperature. The air is eventually dehydrated by condensing water vapour into ice that further precipitates. Different hypotheses of dehydration have been proposed including fast ascent in cumulus clouds (e.g., Danielsen, 1991), slow, large-scale ascent (e.g., Folkins et al., 1999), and convective overshoot followed by a radiatively ascent

ACPD

6, 13001–13025, 2006

(e.g., Sherwood and Dessler, 2000).

The Tropical Convection, Cirrus and Nitrogen Oxides-2 (TROCCINOX-2) campaign took place in the São Paulo state, Brazil in early 2005. Three instrumented research aircrafts were operated to investigate the impact of tropical deep convection on the chemical composition of the troposphere and the lower stratosphere. During the golden day, the 4 February 2005, the mission of the Geophysica stratospheric aircraft was dedicated to thunderstorm interception. Ice particles were observed up to an altitude of 410 K potential temperature, i.e. about 2 km above the local tropopause. Several observational evidences suggest that the particles originated from overshooting plumes that occurred during this severe convective event.

Here this tropical convective event over land is investigated by using a Cloud Resolving Model (CRM). Since a CRM resolves convective circulations, it is able to represent the overshoots with their cloud plumes that are missed by the global models. There are a few three-dimensional (3-D) numerical studies on convective overshoots across the tropopause using CRMs. Most of them consider idealized framework showing cross-tropopause transport via midlatitude deep convection (e.g. Skamarock et al., 2000; Wang, 2003; Mullendore et al., 2005). Some other studies address the impact of convection in the TTL. One case does not produce overshoot penetrating above the cold point (Küpper et al., 2004) while two others found deep overshoots that produce diabatic cooling near the tropopause (Kuang and Bretherton, 2004; Robinson and Sherwood, 2006).

Another novel aspect of the present work is the use of a 3-D quadruply nested numerical simulation initialised with operational weather forecast analyses. The framework of real meteorological conditions allows a direct comparison with the observations taken from the Geophysica along its flight track. In addition, the simulation is evaluated at mesoscale against Meteosat Second Generation (MSG) observations. We adopt a model-to-satellite approach (Morcrette, 1991), in which satellite brightness temperature (BT) images are directly compared to BTs computed from predicted model fields. This approach is especially powerful in identifying discrepancies of cloud cover forecasts

ACPD
6, 13001–13025, 2006

EGU

with BTs at 10.8-µm (Chaboureau et al., 2002). The model-to-satellite approach associated with the BT difference (BTD) technique can also verify specific forecasts such as cirrus cover (Chaboureau and Pinty, 2006) and dust occurrence (Chaboureau et al., 2006). The BTD technique is based on the contrasted absorption property of emitters (gas or particles) at two wavelengths. Hereafter positive BTDs between the 6.2- and 10.8-µm bands is used to identify convective overshoots (Schmetz et al., 1997). As the simulation is sufficiently realistic in reproducing some overshooting plumes, it is used to estimate water vapour and mass fluxes across the tropopause.

The paper is organised as follows. Section 2 describes the model and the experimental design. Section 3 gives an overview of the convective event in both the observation and the simulation. Section 4 describes the overshooting plumes reaching the lower stratosphere. Section 5 presents the estimates of mass and water vapour transport in the lower stratosphere. Section 6 concludes the paper.

2 Model and experimental design

The numerical simulation is performed with the anelastic non-hydrostatic mesoscale model Meso-NH (Lafore et al., 1998). The two-way interactive grid-nesting method (Stein et al., 2000) enables the simultaneous running of several models on the same vertical levels but with different horizontal resolutions. The lateral boundary conditions are given by large-scale European Centre for Medium-Range Weather Forecasts (ECMWF) operational analyses for the outermost model, and they are provided at every time step by the outer models for the inner models.

The case has been simulated with quadruply nested models, with a horizontal grid spacing of 40, 10, 2.5 km , and 625 m. The vertical grid has 90 levels up to 27 km with a level spacing of 40 m close to the surface to 400 m at high altitude. A sponge layer is installed from 22 to 27 km in order to dampen the upward-propagating gravity waves generated by convection. The inner grid covers a domain of about 270 km×210 km centered over São Paulo state in Brazil. The simulation is initialized at 00:00 UTC

ACPD
6, 13001–13025, 2006

EGU

4 February 2005. It is integrated forward for 18 h using the three outer models keeping outputs every hour. At 18:00 UTC, the approximate time of the Geophysica take-off, the simulation is integrated forward for 6 h using the four models keeping outputs every ten minutes. The choice of the model configuration is a trade-off between momentum accuracy and computational expense.

For the two coarser-resolution grids (40 and 10 km), the subgrid-scale convection is parametrized by a mass-flux convection scheme (Bechtold et al., 2001). For the inner grids (2.5 km and 625 m), the convection is explicitly resolved and the convection scheme is switched off. The microphysical scheme includes the three water phases with five species of precipitating and non-precipitating liquid and solid water (Pinty and Jabouille, 1998) with a modified ice to snow autoconversion parameterization following Chaboureau and Pinty (2006). The turbulence parametrization is based on a 1.5-order closure (Cuxart et al., 2000). For the three outer models, the turbulent flux computations are purely vertical using the mixing length of Bougeault and Lacarrère (1989) while for the inner model they are fully three-dimensional based on the parametrization of Deardorff (1974). The radiative scheme is the one used at ECMWF (Gregory et al., 2000) including the Rapid Radiative Transfer Model (RRTM) parameterization (Mlawer et al., 1997). Synthetic BTs corresponding to the MSG observations are computed offline using the Radiative Transfer for Tiros Operational Vertical Sounder (RTTOV) code version 8.7 (Saunders et al., 2005).

3 Overview of the convective event

The time evolution of the convective event is first illustrated by the BT minimum at 10.8-µm in the model-3 domain (Fig. 1). The observed BT minimum displays a diurnal evolution with a maximum of 250 K at 12:00 UTC (09:00 LT) and values less than 220 K before 09:00 UTC and after 15:00 UTC. At 14:00 UTC, the minimum BT drops 35 K in one hour characterizing the triggering of deep convection. The time evolution is typical of the convection over land with a regime of deep convection in

ACPD
6, 13001–13025, 2006

the afternoon (e.g. Chaboureau et al., 2004). A massive amount of convective available potential energy (CAPE) is present with maximum values larger than 3800 J kg^{-1} at 16:00 UTC. Once deep convection is triggered, the coldest clouds occur between 18:00 and 21:00 UTC (during the Geophysica flight). The diurnal evolution is rather well reproduced by the simulation. A minimum of 187 K (−86 °C) is observed between 18:00 and 22:00 UTC while the simulation records 186 K at 19:00 UTC. The close time evolution of the convective events between the simulation and the MSG observation is confirmed at each hour (e.g. see Fig. 3). Note that this case occurred in a period with few organized convection over the São Paulo state and it was well forecasted in real time during the TROCCINOX campaign by the Meso-NH model when operating in a regional mode with an horizontal grid mesh of 30 km (Chaboureau and Pinty, 2006).

The realism of the simulation is further illustrated with measurements obtained by the Fluorescent Advanced Hygrometer (FLASH) and the Forward Scattering Spectrometer Probe (FSSP)-100 on board the Geophysica. The FLASH instrument is based on the Lyman-α fluorescence technique with an average time of 1 s and an accuracy of 0.2 µmol mol^{-1} (or ppmv). The FSSP-100 is a laser-particle spectrometer that samples the size distribution of aerosols between 0.4 and 40 µm every 20 s with an accuracy of 20%. The observed and simulated relative humidity with respect to ice as well as the total particle concentration recorded along the Geophysica flight are displayed in Fig. 2. The potential temperature is also shown to give an indication of the altitude.

On first ascent, the Geophysica reached the altitude of 18.7 km allowing us to characterize the TTL. Following the climatology study of Gettelman and Forster (2002), the TTL can be locally defined as extending from the level of the lapse rate minimum at 10–12 km to the cold-point tropopause (CPT) at 16–17 km. When applied to the Geophysica observations, these criteria put the TTL base around 12 km and its top at 17.2 km with a CPT of −82.8 °C and a potential temperature of 378 K. However, at 16.3 km both temperature and water vapour experience a strong change in their vertical gradient, with local minima of −80.0 °C and 3 ppmv, respectively. Therefore the 16.3 km altitude (or 362-K potential temperature) hereafter defines the TTL top while

the value of −80.0 °C is taken as the environmental CPT.

Two ascents within the lower stratosphere were decided by the pilot in order to flight over huge clouds. They are indicated with the vertical dashed lines, around 18:20 UTC (66 000 s) and 20:30 UTC (73 800 s). During these two ascents, ice particles were probe by the FSSP-100 up to an altitude of 410 K, i.e. about 2 km above the local tropopause. The decrease of relative humidity detected by the FLASH hygrometer from 60% to 20% during the first ascent is correctly reproduced by the simulation. But at 20:30 UTC the 40% simulated relative humidity is much lower than the 60% observed. The particles found in subsaturated air suggest they originate from overshooting air parcels that mix with stratospheric dry air.

Between the two ascents, the Geophysica flew over a distance of 1500 km between 360 and 378 K, i.e. the TTL top and the CPT level. Supersaturation with respect to ice is observed up to 200% with occasional presence of ice. In the simulation, saturation is sometimes achieved, but without any supersaturation as the bulk microphysics parameterization imposes a humidity adjustment to saturation. Furthermore, saturation is less frequently simulated than observed. This might be explained by expected differences in locations of the convective ascents between observation and simulation. In conclusion, the direct comparison with the Geophysica observations provides a fair qualitative agreement.

The convective event is now investigated at mesoscale by using satellite observations. Here the results are shown over the model-3 domain whose grid spacing (2.5 km) corresponds to the MSG resolution (about 3.5 km over the São Paulo state). Observed and simulated MSG BT at 10.8-µm are displayed at 18:30 and 20:30 UTC when ice particles were detected above 390 K (Fig. 3). The cloud systems sampled by the Geophysica are characterized by 10.8-µm BT less than 193 K (−80 °C), the coldest clouds being the thickest and the deepest. The main cloud system is organized along a line that evolves from the northwest-southeast to a zonal direction in two hours. In addition, convective overshoots are identified using satellite imagery with BTDs between the 6.2- and 10.8-µm larger than 3 K. Larger BTs at 6.2-µm than at 10.8-µm are ex-

ACPD
6, 13001–13025, 2006

EGU

plained by stratospheric water vapour, which absorbs radiation from the cold cloud top and emits radiation at higher stratospheric temperatures (Schmetz et al., 1997). The 3-K threshold has been arbitrarily chosen to highlight the BTD signature. It is less than the empirical value of 5 K used by Roca et al. (2002) to analyse deep convection over the Indian Ocean. During the two particular Geophysica flight legs, BTDs over this particular threshold are effectively found over the coldest clouds where particles are observed in the lower stratosphere.

The simulated low BTs at 10.8-µm present a line pattern similar to the observed ones (Fig. 3). However, there is not exact matching between the observed and the simulated individual cells, as also seen from the comparison along the flight track. For example, the westernmost cloud systems are missing. This might be ascribed to the absence of smaller mesoscale features in the initial conditions and surface forcing. In the central part of the domain, the simulated convective cells appear to be more scattered at 18:30 UTC than observed resulting in a cluster at 20:30 UTC with larger BT minimum. This suggests a poor representation of the turbulent mixing between the in-cloud air and its environment. This is to be expected from a simulation with a 625-m horizontal grid spacing partly resolving turbulent fluxes of water vapour (e.g. Petch et al., 2002; Bryan et al., 2003; Petch, 2006). Finally convective overshoots (as seen by BTDs larger than 3 K) are also simulated over the coldest clouds of several individual cells within and outside the model-4 domain (Fig. 3). In summary, the simulation reproduces reasonably well the convective event.

4 Overshooting plumes

The simulated overshooting plumes are now investigated in the inner model (with a 625-m horizontal grid spacing). At 18:30 UTC many cells reach the tropopause as seen with 10.8-µm BT less than 193 K (Fig. 4). The coldest cloud tops are characterized with both water vapour mixing ratio at 390 K larger than the background values of 4 ppmv (black isoline) and BTDs between the 6.2- and 10.8-µm larger than 3 K (red

ACPD
6, 13001–13025, 2006

EGU

isoline). The two fields do not exactly match as the former is a water vapour amount at a certain level while the latter is sensitive to the relative humidity (temperature and water vapour) integrated over the atmospheric column above the cloud top. This suggests that the BTD signal is an interesting indicator of water vapour anomalies in the stratosphere above the cloud tops reaching the cold point. Future work is needed to investigate the relationship between the BTD magnitude and the stratospheric water vapour anomalies. Such a radiative measure from space would further characterize the water vapour transport across the tropopause.

The time evolution of the maximum vertical velocities inside the inner model is now examined (Fig. 5). A maximum of 76 m s^{-1} is reached at 18:20 UTC. Such dramatic values have been reported for mid-latitude deep convective events with different CAPE amounts. Maximum vertical velocities of 50–55 m s^{-1} have been observed for a 3-D simulated deep supercell storm starting from a sounding of 3012 J kg^{-1} CAPE (Wang, 2003). Mullendore et al. (2005) obtained a maximum of 88 m s^{-1} with a 1-km horizontal grid spacing 3-D simulation initialized with a sounding of very high CAPE (5034 J kg^{-1}). The latter fairly reproduces a deep convective event with overshooting cloud tops reaching 18–19 km over Kansas where the tropopause height was at 13.5 km. Under tropical conditions, Robinson and Sherwood (2006) run a series of 2-D simulations with increasing initial heating sources. As expected, the larger the CAPE, the higher the vertical velocity. Their simulation with a maximum CAPE of 3520 J kg^{-1} is characterized by a maximum of 55 m s^{-1}. After 18:20 UTC the maximum vertical velocities unevenly decreases with time. The several secondary maximum updraughts that occur every 60–80 min are the signature of separate cells growing and dissipating as shown by the maximum values for the different boxes (whose frames are displayed in Fig. 4). In box 5, the absolute maximum value of 76 m s^{-1} appears to be due to the interaction between two cells (not shown). Also at 18:20 UTC a second maximum value of 62 m s^{-1} is obtained in box 2, but due to a single cell.

The convective event associated with the individual plume in box 2 is detailed with a series of vertical cross sections along the mean stratospheric flow (Fig. 6). At

ACPD
6, 13001–13025, 2006

EGU

18:10 UTC an updraught from 3 to 18 km is already established resulting a plume of total water larger than 2 g kg^{-1} standing up to 15 km, a cloud top just below 370 K, and an outflow at 14 km (as depicted by the 10^{-3} kg kg^{-1} red line). The diabatic heating within the updraught results in a 4-km lowering of the 350-K isentrope. The environment, already perturbed by previous convective activities, is characterized by a vertical decrease of the total water, with two remarkable values, 5 g kg^{-1} near the freezing level (around 4–5 km) and 0.25 g kg^{-1} (around 4 ppmv) at 370 K. (This 4 ppmv background value comes from the ECMWF analysis and is slightly larger than the 3 ppmv measured during the first Geophysica ascent.) At 18:20 UTC the updraught attains its climax with the vertical plume and its associated cloud cover reaching 19 km. The layer between 350 and 370 K has doubled in thickness. At 17 km the rising air is first adiabatically cooled resulting in a mean decrease of the CPT to −88°C. The saturation mixing ratio is sufficiently reduced so that could locally yield to air dehydration where ice sedimentation is fast enough. But the vertical motion is so strong that ascending air cross isentropes in the lower stratosphere.

At 18:30 UTC the updraught is ended leaving a perturbed circulation. In the troposphere below 15 km, many rotors mix environmental air with the cloud. In the lower stratosphere the cloud top drifted 6 km westward with water vapour larger 4 ppmv found up to 20 km. At 18:40 and 18:50 UTC the atmosphere continues to recover from the convective burst, the cloud dissipates by precipitation and mixing. In the lower stratosphere, water vapour anomalies over 0.37 g kg^{-1} (around 6 ppmv) remain. Finally at 19:00 UTC the cloud top is at 17 km all along the cross section. Within the troposphere, the dissipation of cloud by hydrometeor precipitation continues. Above the cloud cover, between 17 and 20 km, the pockets of water vapour anomalies have been stretched into thin layers with mixing ratio larger than 6 ppmv. This clearly shows that an individual overshooting plume can transport and deposit moisture into the stratosphere.

ACPD
6, 13001–13025, 2006

EGU

5 Mass and water vapour transport

The impact of such a deep convective event on the composition of the stratosphere is now discussed. The cross-isentropic water vapour transport is given over the model-3 domain. The transport of water vapour is calculated by summing the values of positive vertical flux across isentropic surface for different values of potential temperature. As expected, the resulting water vapour fluxes are the largest at 19:00 UTC and these maximum values decrease with increasing potential temperature (Fig. 7). It is worth noting that the peak value of 8 tons s^{-1} obtained across the 380-K surface matches the simulated value by Wang (2003) for a north-American Midwest severe thunderstorm.

Further estimate of the total mass flux is displayed in Fig. 8 following the presentation of Küpper et al. (2004). The mass flux derived from the simulation has been obtained after averaging over the model-3 domain and over the 24 h of the simulation. The results derived from previous studies are also shown. All the mass flux estimates show decreasing values with altitude, but for different ranges within the TTL. The present CRM results is an upper bound to those derived from O_3 and CO budgets by Dessler (2002) indicating that convection transport mass at the tropopause. These estimates are two orders of magnitude greater than the mass flux obtained by Küpper et al. (2004) from a CRM simulation (run to a radiative-convective equilibrium) representative of maritime conditions. The present estimate is also larger than the one obtained from cloud imagery and reanalysis temperatures by Gettelman et al. (2002). Based on BTs at 11 µm colder than the tropopause, they found that convection rarely penetrates more than 1.5 km above the tropopause.

However, recent studies on tropical overshoots have shown that these cases are not so infrequent. Liu and Zipser (2005) use a 5-year Tropical Rainfall Measuring Mission (TRMM) database to detect large ice particles lifted that overshoot. Their overshooting criteria search for 20 km^2 pixels with more than 20 dBZ of radar reflectivity above a reference height. They found that 1.3% of tropical convection systems reach 14 km and 0.1% of them may even penetrate the 380-K potential temperature level. Furthermore

ACPD
6, 13001–13025, 2006

EGU

stronger overshooting is found over land, including South America (Liu and Zipser, 2005). Another study from Geoscience Laser Altimeter System (GLAS) observations find more frequent occurrence of thick clouds in the TTL and above the tropopause than other studies due to the high spatial resolution of the lidar, with 76.8 m in the vertical and 1.4 km in the horizontal. Dessler et al. (2006) found that 3.0% and 19% of the thick and thin cloud observations, respectively, show a cloud top in the TTL and 0.34% and 3.1% show a cloud top above the average level of the tropopause.

Finally, in absence of vertical shear, the individual event studied here remains localized. A satellite analysis of convective systems over Indian Ocean shows that for mesoscale organized convection (spanning an area larger than 10^4 km^2) the larger the deepest systems the larger the fraction of overshoot areas (Roca et al., 2002). It is anticipated that more import of water vapour in the stratosphere should be find over organized systems as it was observed during the African Monsoon Multidisciplinary Analysis (AMMA) campaign (J.-P. Pommereau 2006, personal communication).

6 Conclusions

The paper presents a numerical study of the TROCCINOX golden day. For the first time in the framework of real meteorological conditions, a tentative estimate of mass fluxes across the TTL is given for a tropical case simulated by a CRM. Comparisons with observations show the good overall quality of the simulation. The convective event build-up in time with minimum BT at 10.8-µm between 18:00 and 21:00 UTC. In particular, the BT minimum of 187 K is reproduced, a value 6 K colder than the environmental cold-point temperature. At local scale, the moisture variation measured during the Geophysica flight is captured. At mesoscale the thickest and deepest clouds are correctly organized in line with overshooting cells and positive BTD between the 6.2- and 10.8-µm bands on the top. Moreover, a simulated overshoot supports the explanation for the presence of particles up to 410 K. Upward water vapour mass fluxes are of the same order of magnitude than those of a midlatitude case. Day-averaged mass

ACPD
6, 13001–13025, 2006

fluxes derived from the simulation are also consistent with a global budget study. All these elements support the scenario of deep convective overshoots from troposphere-stratosphere exchange.

This numerical study however suffers from uncertainties that need to be alleviated. First, the framework of real meteorological conditions imposes the simulation with grid mesh of few hundred meters. This may result in a poor representation of the turbulent mixing between the in-cloud air and its environment within the troposphere, and the gravity wave breaking aloft. Therefore higher-resolution simulation will be run under idealized framework. Then the cloud microphysics used here can not allow supersaturation to occur, in contradiction with the observations in the upper troposphere. This may result in an excess of latent heat release by condensation. The sensitivity to a more elaborate cloud scheme, like a double-moment scheme, will require further study. Finally the use of passive tracers would give a more quantitative cross-tropopause transport in such a very intense deep convective event. The coming idealized case study will take benefit from measurements that have been not used here, such as trace gases, aerosol profiles, and lightning activity. The present case represents a single tropical convective event. A higher wind shear environment would enhance the cross-tropopause transport by breaking wave more easily in the stratosphere. There is a strong need to study such case (e.g. squall line and other tropical mesoscale convective systems). Another critical numerical issue concerns the fate of positive water vapour anomalies after the stratospheric penetration. This issue could be addressed with the combination of high-resolution run and large-scale models only, that under the framework of superparametrization or global (at least regional) CRM runs during sufficiently long periods.

Acknowledgements. We are grateful to J.-P. Pinty for his helpful comments. This research was supported by the TROCCINOX project funded by the European Commission under the contract EVK2-CT-2001-00122. Computer resources were allocated by IDRIS. MSG observations have been delivered by SATMOS.

References

Bechtold, P., Bazile, E., Guichard, F., Mascart, P., and Richard, E.: A mass flux convection scheme for regional and global models, Quart. J. Roy. Meteor. Soc., 127, 869–886, 2001. 13005

Bougeault, P. and Lacarrère, P.: Parameterization of orographic induced turbulence in a meso-betascale model, Mon. Weather Rev., 117, 1872–1890, 1989. 13005

Bryan, G. H., Wyngaard, J. C., and Fritsch, J. M.: Resolution requirements for the simulation of deep moist convection, Mon. Weather Rev., 131, 2394–2416, 2003. 13008

Chaboureau, J.-P. and Pinty, J.-P.: Evaluation of a cirrus parameterization with Meteosat Second Generation, Geophys. Res. Lett., 33, L03 815, doi:10.1029/2005GL024 725, 2006. 13004, 13005, 13006

Chaboureau, J.-P., Cammas, J.-P., Mascart, P., Pinty, J.-P., and Lafore, J.-P.: Mesoscale model cloud scheme assessment using satellite observations, J. Geophys. Res., 107(D17), 4301, doi:10.1029/2001JD000 714, 2002. 13004

Chaboureau, J.-P., Guichard, F., Redelsperger, J.-L., and Lafore, J.-P.: The role of stability and moisture in the development of convection, Quart. J. Roy. Meteor. Soc., 130, 3105–3117, 2004. 13006

Chaboureau, J.-P., Tulet, P., and Mari, C.: Diurnal cycle of dust and cirrus over West Africa as seen from Meteosat Second Generation satellite and a regional forecast model, Geophys. Res. Lett., 33, doi:10.1029/2006GL027 771, in press, 2006. 13004

Cuxart, J., Bougeault, P., and Redelsperger, J.-L.: A turbulence scheme allowing for mesoscale and large-eddy simulations, Quart. J. Roy. Meteorol. Soc., 126, 1–30, 2000. 13005

Danielsen, E. F.: In situ evidence of rapid, vertical, irreversible transport of lower tropospheric air into the lower tropical stratosphere by convective cloud turrets and by larger-scale upwelling in tropical cyclones, J. Geophys. Res., 98(D5), 8665–8681, 1991. 13002

Deardorff, J. W.: Three-dimensional numerical study of turbulence in an entraining mixed layer, Bound. Layer. Meteor., 7, 199–216, 1974. 13005

Dessler, A. E.: The effect of deep, tropical convection on the tropical tropopause layer, J. Geophys. Res., 107(D3), 4033, doi:10.1029/2001JD000 511, 2002. 13011, 13025

Dessler, A. E., Palm, S. P., and Spinhirne, J. D.: Tropical cloud-top height distributions revealed by the Ice, Cloud, and Land Elevation Satellite (ICESat)/Geoscience Laser Altimeter System (GLAS), J. Geophys. Res., 111, D12 215, doi:10.1029/2005JD006 705, 2006. 13012

Etheridge, D. M., Steele, L. P., Francey, R. J., and Langenfelds, R. L.: Atmospheric methane between 1000 A.D. and present: Evidence of anthropogenic emissions and climatic variability, J. Geophys. Res., 103(D13), 15 979–15 994, 1998. 13002

Folkins, I., Loewenstein, M., Podolske, J., Oltmans, S. J., and Proffitt, M.: A barrier to vertical mixing at 14 km in the tropics: Evidence from ozonesondes and aircraft measurements, J. Geophys. Res., 104(D18), 22 095–22 102, 1999. 13002

Gettelman, A. and Forster, P. M. D. F.: Definition and climatology of the tropical tropopause layer, J. Meteor. Soc. Japan, 80, 911–924, 2002. 13006

Gettelman, A., Salby, M. L., and Sassi, F.: Distribution and influence of convection in the tropical tropopause region, J. Geophys. Res., 107 (D10): Art. No. 408026, 1601–1604, 2002. 13011, 13025

Gregory, D., Morcrette, J.-J., Jakob, C., Beljaars, A. M., and Stockdale, T.: Revision of convection, radiation and cloud schemes in the ECMWF model, Quart. J. Roy. Meteor. Soc., 126, 1685–1710, 2000. 13005

Kuang, Z. and Bretherton, C. S.: Convective influence on the heat balance of the tropical tropopause layer: a cloud-resolving model study, J. Atmos. Sci., 61, 2919–2927, 2004. 13003

Küpper, C., Thuburn, J., Craig, G. C., and Birner, T.: Mass and water transport into the tropical stratosphere: A cloud-resolving simulation, J. Geophys. Res., 109, D10 111, doi:10.1029/2004JD004 541, 2004. 13003, 13011, 13025

Lafore, J.-P., Stein, J., Asencio, N., Bougeault, P., Ducrocq, V., Duron, J., Fischer, C., Héreil, P., Mascart, P., Masson, V., Pinty, J.-P., Redelsperger, J.-L., Richard, E., and Vilà-Guerau de Arellano, J.: The Meso–NH Atmospheric Simulation System. Part I: adiabatic formulation and control simulations. Scientific objectives and experimental design, Ann. Geophys., 16, 90–109, 1998, http://www.ann-geophys.net/16/90/1998/. 13004

Liu, C. and Zipser, E. J.: Global distribution of convection penetrating the tropical tropopause, J. Geophys. Res., 110, D23 104, doi:10.1029/2005JD006 063, 2005. 13011, 13012

Mlawer, E. J., Taubman, S. J., Brown, P. D., Iacono, M. J., and Clough, S. A.: Radiative transfer for inhomogeneous atmospheres: RRTM, a validated corrolated-k model for the longwave, J. Geophys. Res., 102D, 16 663–16 682, 1997. 13005

Morcrette, J.-J.: Radiation and cloud radiative properties in the European centre for medium range weather forecasts forecasting system, J. Geophys. Res., 96, 9121–9132, 1991. 13003

Mullendore, G. L., Durran, D. R., and Holton, J. R.: Cross-tropopause tracer transport in midlatitude convection, J. Geophys. Res., 110, D06 113, doi:10.1029/2004JD005 059.536–549, 2005. 13003, 13009

Oltmans, S. J., Vömel, H., Hofmann, D. J., Rosenlof, K. H., and Kley, D.: The increase in stratospheric water vapor from balloonborne, frostpoint hygrometer measurements at Washington, D.C., and Boulder, Geophys. Res. Lett., 27(21), 3453–3456, 2000. 13002

Petch, J.: Sensitivity studies of developing convection in cloud-resolving model, Quart. J. Roy. Meteor. Soc., 132, 345–358, 2006. 13008

Petch, J. C., Brown, A. R., and Gray, M. E. B.: The impact of horizontal resolution on convective development in simulations of the diurnal cycle over land, Quart. J. Roy. Meteor. Soc., 128, 2031–2044, 2002. 13008

Pinty, J.-P. and Jabouille, P.: A mixed-phase cloud parameterization for use in a mesoscale non-hydrostatic model: simulations of a squall line and of orographic precipitations, in: Proc. AMS conference on cloud physics, 17–21 August 1998, Everett, Wa, USA, pp. 217–220, 1998. 13005

Robinson, F. J. and Sherwood, S. C.: Modeling the impact of convective entrainment on the tropical tropopause, J. Atmos. Sci., 63, 1013–1027, 2006. 13003, 13009

Roca, R., Viollier, M., Picon, L., and Desbois, M.: A multi satellite analysis of deep convection and its moist environment over the Indian Ocean during the winter monsoon, J. Geophys. Res., 107, 10.1029/2000JD000 040, 2002. 13008, 13012

Rosenlof, K. H. I., Chiou, E.-W., Chu, W. P., Johnson, D. G., Kelly, K. K., Michelsen, H. A., Nedoluha, G. E., Remsberg, E. E., Toon, G. C., and McCormick, M. P.: Stratospheric water vapor increases over the past half-century, Geophys. Res. Lett., 28(7), 1195–1198, 2001. 13002

Saunders, R., Matricardi, M., Brunel, P., English, S., Bauer, P., O'Keeffe, U., Francis, P., and Rayer, P.: RTTOV-8 Science and validation report, Tech. rep., NWP SAF Report, 41 p., 2005. 13005

Schmetz, J., Tjemkes, S. A., Gube, M., and van de Berg, L.: Monitoring deep convection and convective overshooting with METEOSAT, Adv. Space Res., pp. 433–441, 1997. 13004, 13008

Sherwood, S. C. and Dessler, A. E.: On the control of stratospheric humidity, Geophys. Res. Lett., 58, 2513–2516, 2000. 13003

Skamarock, W. C., Powers, J. G., Barth, M., Dye, J. E., Matejka, T., Bartels, D., Baumann,

K., Stith, J., Webster, C. R., Grecu, J., Loewenstein, M., Podolske, J. R., Parrish, D. D., and Hubler, G.: Numerical simulations of the 10 July Stratospheric-Tropospheric Experiment: Radiation, Aerosols, and Ozone/Deep Convection Experiment convective system: Kinematics and transport, J. Geophys. Res., 105(D15), 19 973–19 990, 2000. 13003

Stein, J., Richard, E., Lafore, J.-P., Pinty, J.-P., Asencio, N., and Cosma, S.: High-resolution non-hydrostatic simulations of flash-flood episodes with grid-nesting and ice-phase parameterization, Meteorol. Atmos. Phys., 72, 203–221, 2000. 13004

Wang, P. K.: Moisture plumes above thunderstorm anvils and their contributions to cross-tropopause transport of water vapor in midlatitudes, J. Geophys. Res., 108(D6), 4194, doi:10.1029/2002JD002 581, 2003. 13003, 13009, 13011

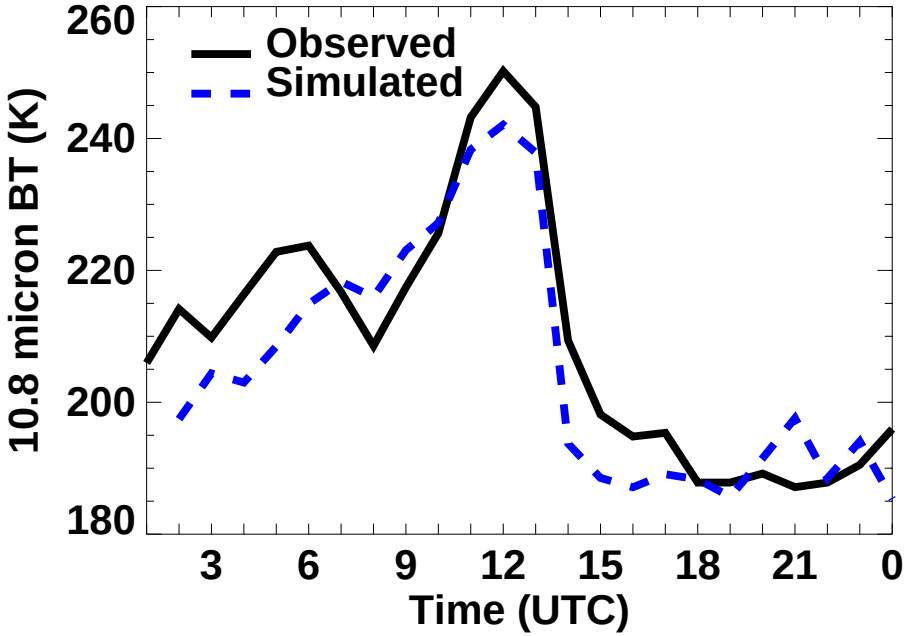

Fig. 1. Time evolution of observed and simulated minimum BT (K) at 10.8 μm in the model-3 domain. The temporal resolution is 1 h.

ACPD
6, 13001–13025, 2006

EGU

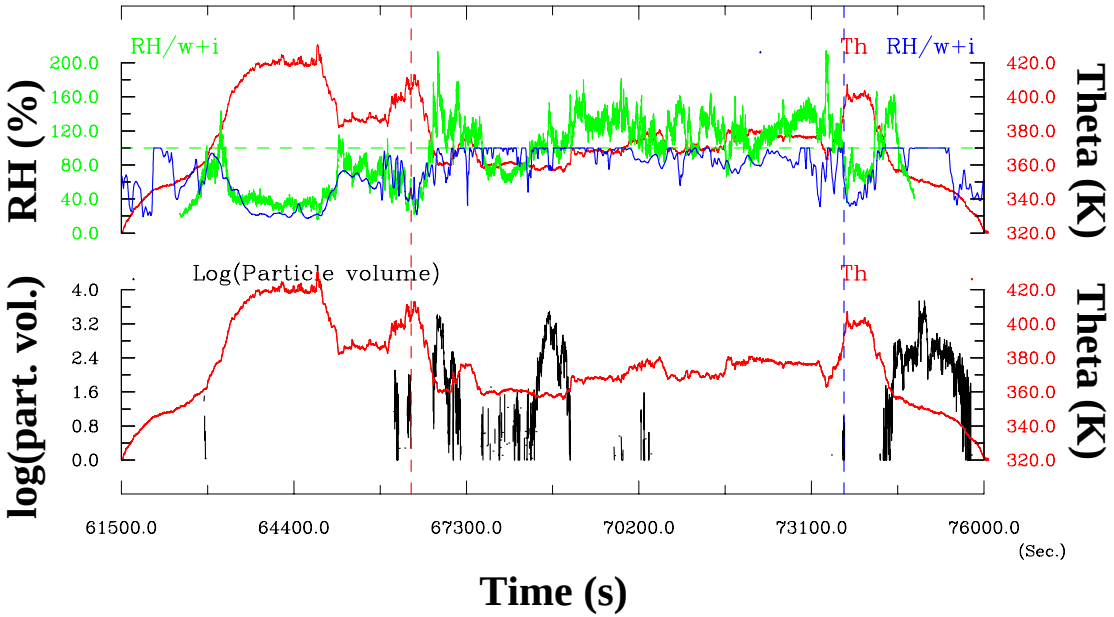

Fig. 2. Top: observed potential temperature (red line, K), relative humidity (green line, %) and simulated relative humidity (blue line, %) during the Geophysica flight. Bottom: observed potential temperature (red line, K) and total particle concentration (black line, cm^3) as measured by the FSSP-100 instrument. The horizontal axis is the time in s.

ACPD
6, 13001–13025, 2006

EGU

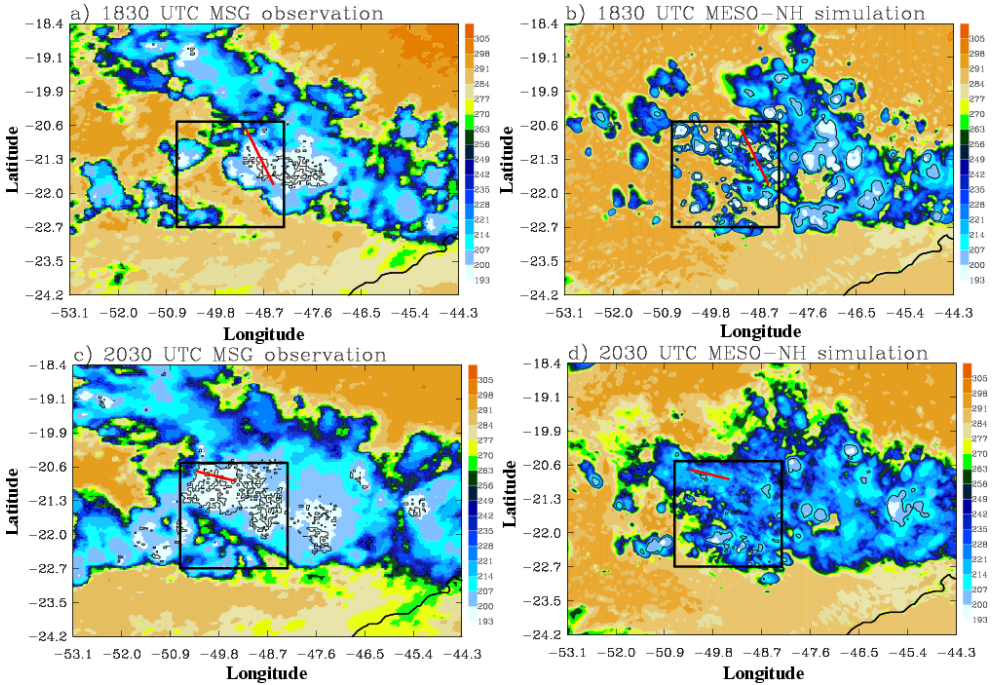

Fig. 3. (Left) Observed and (right) simulated MSG BTs over the model-3 domain at (top) 18:30 UTC and (bottom) 20:30 UTC 4 February 2005. The colour scale indicates BT at 10.8 µm. The 3-K isoline of the BTD between 6.2- and 10.8 µm band is superimposed. The red lines in the top and bottom panels indicate the Geophysica flight track between 18:15–18:30 UTC and 20:15–20:30 UTC, respectively. The square shows the location of the model 4 domain.

ACPD
6, 13001–13025, 2006

EGU

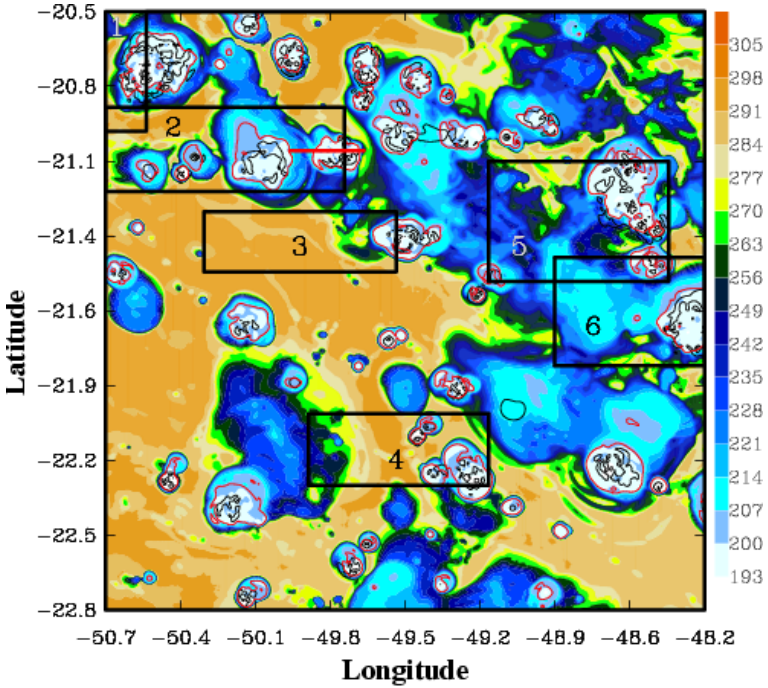

Fig. 4. High-resolution simulated fields in the model 4 domain at 18:30 UTC: BT at 10.8 μm (color, K), BTD between 6.2- and 10.8 μm band (3-K isoline in red), and water vapour mixing ratio over a 390-K potential temperature surface (4-ppmv isoline in black). The boxes indicate different sub-domains with occurrence of overshoots. The red line gives the position of the vertical cross-sections in Fig. 6.

ACPD
6, 13001–13025, 2006

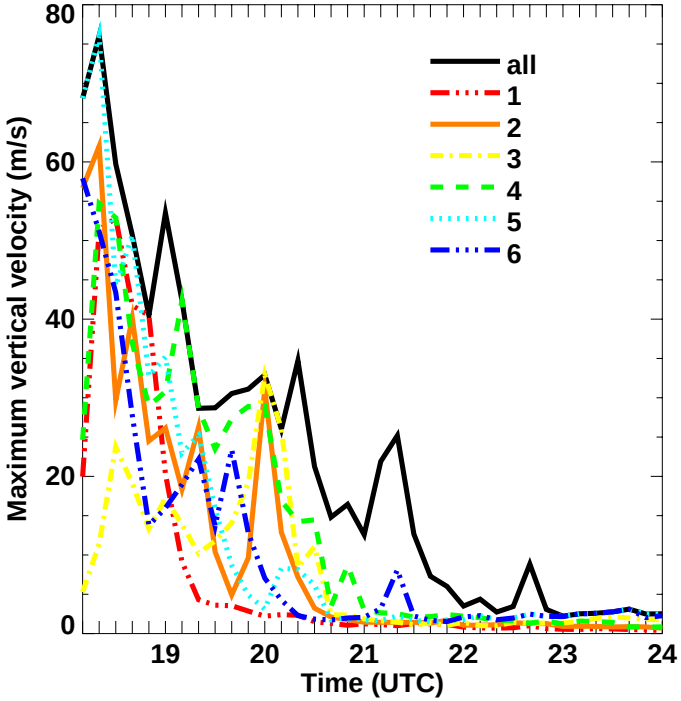

Fig. 5. Time evolution of the vertical velocity maximum ($m\,s^{-1}$). The results are given from the inner model for the whole domain and 6 boxes shown in Fig. 4. The temporal resolution is 10 min.

ACPD
6, 13001–13025, 2006

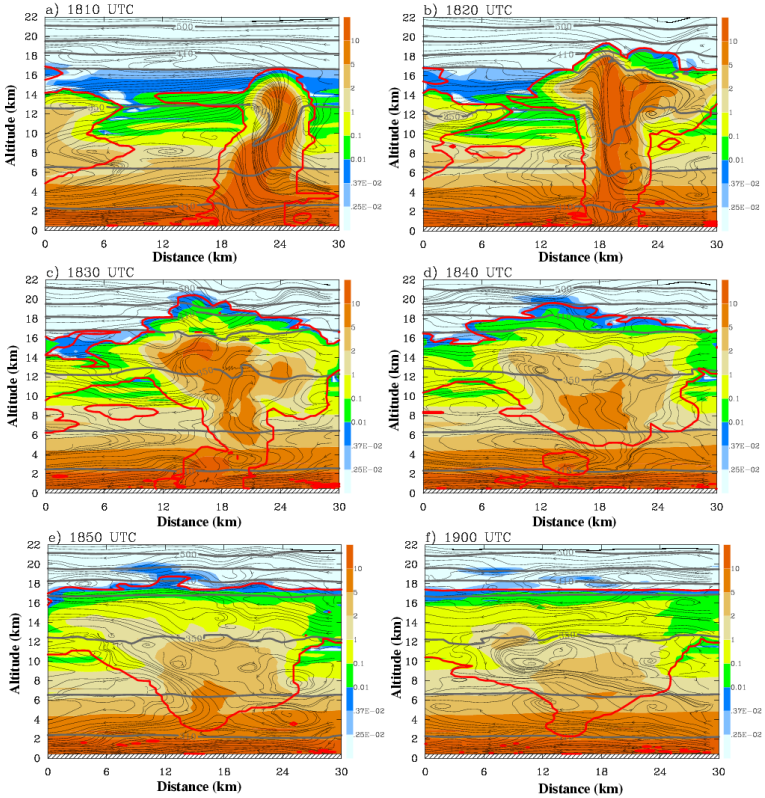

Fig. 6. Vertical cross section of the total water mixing ratio ($g\,kg^{-1}$) at 18:10, 18:20, 18:30, 18:40 18:50, and 19:00 UTC 4 February 2005 along the line shown in Fig. 4. Black lines are the streamfunctions along the cross-section. Grey contours represent potential temperatures (intervals 310, 330, 350, 370, 410, 450, and 500 K). The red line delineates the cloud limit with condensed water mixing ratio larger than $10^{-3}\,kg\,kg^{-1}$. The vertical axis range is 0–22 km and horizontal axis range 0–30 km. The aspect ratio is 1.

ACPD
6, 13001–13025, 2006

EGU

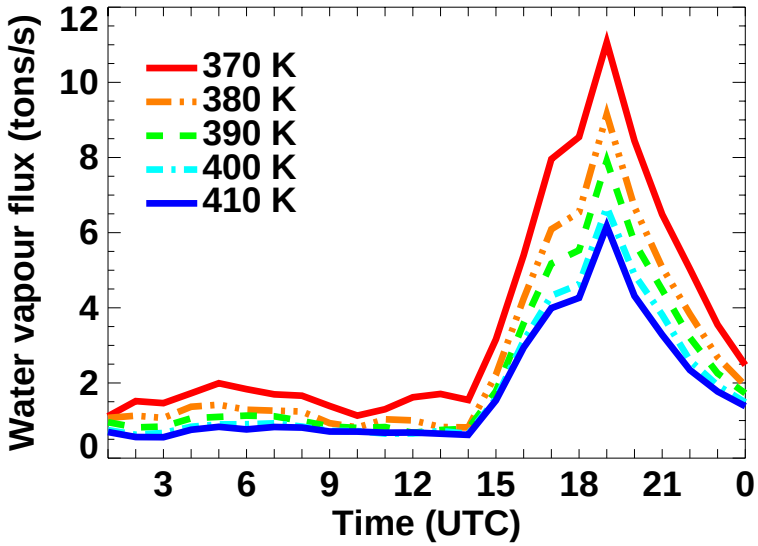

Fig. 7. Times series of upward water vapour flux through isentropic surface of 370, 380, 390, 400, and 410 K over the model-3 domain. The temporal resolution is 1 h.

ACPD
6, 13001–13025, 2006

EGU

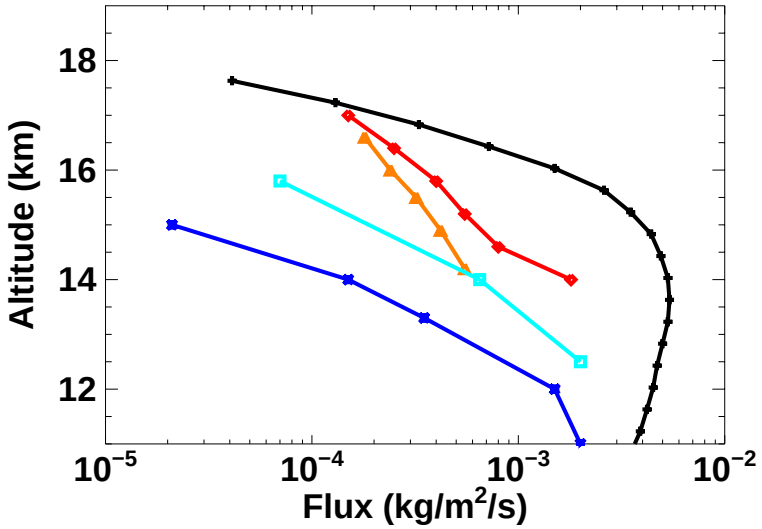

Fig. 8. Mass flux estimates based on O_3 (red diamonds) and CO (orange triangles) budgets (Dessler, 2002), cloud imagery (cyan squares; Gettelman et al., 2002), and cloud-resolving simulation from Küpper et al. (2004) (blue asteriks) and this work (black crosses).

ACPD
6, 13001–13025, 2006

EGU